

An independent distortional analysis method of thin-walled multicell box girders

Nam-Hoi Park[†] and Young-Jong Kang[‡]

Department of Civil and Environmental Engineering, Korea University, 5-1, Anam-Dong, Sungbuk-Ku, Seoul 136-701, South Korea

Hee-Joong Kim^{‡†}

Department of Civil Engineering, Keimyung University, 1000, Shindang-Dong, Dalseo-Ku, Daegu 704-701, South Korea

(Received October 8, 2004, Accepted July 29, 2005)

Abstract. When a thin-walled multicell box girder is subjected to an eccentric load, the distortion becomes an important global response in addition to flexure and torsion. The three global responses appear in a combined form when a conventional shell element is used thus it is not an easy task to examine the three global responses separately. This study is to propose an analysis method using conventional shell element in which the three global responses can be separately decomposed. The force decomposition method which was designed for a single-cell box girder by Nakai and Yoo is expanded herein to multicell box girders. The eccentric load is decomposed in the expanded method into flexural, torsional, and multimode distortional forces by using the force equilibrium. From the force decomposition, the combined global responses of multicell box girders can be resolved into separate responses and the distortional response which is of primary concern herein can be obtained separately. It is shown from a series of extensive comparative studies using three box girder bridge models that the expanded method produces accurate decomposed results. Noting that the separate consideration of individual global response is of paramount importance for optimized multicell box girder design, it can be said that the proposed expanded method is extremely useful for practicing engineers.

Key words: independent distortional analysis; shell analysis; force decomposition; expanded method; multicell box girders.

1. Introduction

The study related to the distortional analysis of box girders was initiated by Dabrowski (1968), who first explained the distortional phenomenon of single-cell box members with a symmetric cross-section. Since then, researches associated with distortional analyses of multicell box girders have been performed by several investigators (Sedlacek 1968, Maisel 1970, 1985, Zhang and Lyons

[†] Research Professor

[‡] Professor, Corresponding author, E-mail: yjkang@korea.ac.kr

^{‡†} Associate Professor

1984, Razaqpur and Li 1991, 1994, Jonsson 1999). However, the previous researches were limited to the distortional analysis using box beam elements. The analysis using the box beam elements requires the preliminary computation of the distortion-related section-properties such as the distortional center, the distortional warping function, the distortional stiffness, and so on, which is extremely difficult for practicing engineers.

Nowadays, many conventional shell elements are available in most of commercial finite element programs. Therefore, the use of the conventional shell element may become an excellent alternate resort to the distortional analysis of box girders. One of the most important advantages of using the shell element is that the complex section-properties need not be computed. The shell element analysis, which once was not practical owing to the vast amount of computational time and memory, has become considerably facilitated these days thanks to rapid development of high performance computers. However, when a box girder subjected to an eccentric load is analyzed using shell element, the responses corresponding to global behavior such as flexure, torsion, and distortion are presented in such a combined form that individual responses can hardly be examined. Unfortunately, any study has not been reported up to date for separate distortional analysis using shell elements. Since the examination of individual responses is extremely important for optimal proportioning of box girders, the development of an analysis method in which the global responses of flexure, torsion, and distortion are separately presented is urgently needed.

Presented for this purpose in the present study is an expanded method for multicell box girders analysis using conventional shell elements. The force decomposition method which was designed for a single-cell box girder by Nakai and Yoo (1988) is expanded herein to multicell box girders. The eccentric load is decomposed in the expanded method into flexural, torsional, and multimode distortional forces by using the force equilibrium. From the force decomposition, the combined global responses of multicell box girders can be resolved into separate responses and the distortional response which is of primary concern herein can be obtained separately.

The proposed expanded method consists of three independent analyses as follows; an independent flexural analysis, an independent torsional analysis, and independent multimode distortional analyses. In order to verify the proposed expanded method, three box girder bridge models were selected. The box cross-section is limited to rectangular shapes of singly or doubly symmetric sections. It is shown from a series of extensive comparative studies using the distortional displacement, the distortional warping normal stress, and the transverse bending normal stress that the expanded method produces accurate and conveniently decomposed results.

The spacing requirement of intermediate diaphragms in a box girder is to limit the ratio of the distortional warping normal stress to the bending normal stress and to limit the transverse bending normal stress to a specified value (AASHTO 1993, Hanshin Express Public Corporation of Japan 1988). Noting that accurate individual response evaluation of flexure, torsion, and distortion is of paramount importance for appropriate proportioning of multicell box girders, it can be said that an extremely effective method is proposed herein for practicing engineers.

2. Distortion of single-cell box girders

Before discussing multicell box girders, distortional behavior of box girders with a single-cell cross-section is briefly explained in this section. As shown in Fig. 1, when a single-cell box girder is subjected to an eccentric load p , the load can be resolved into flexural and torsional forces

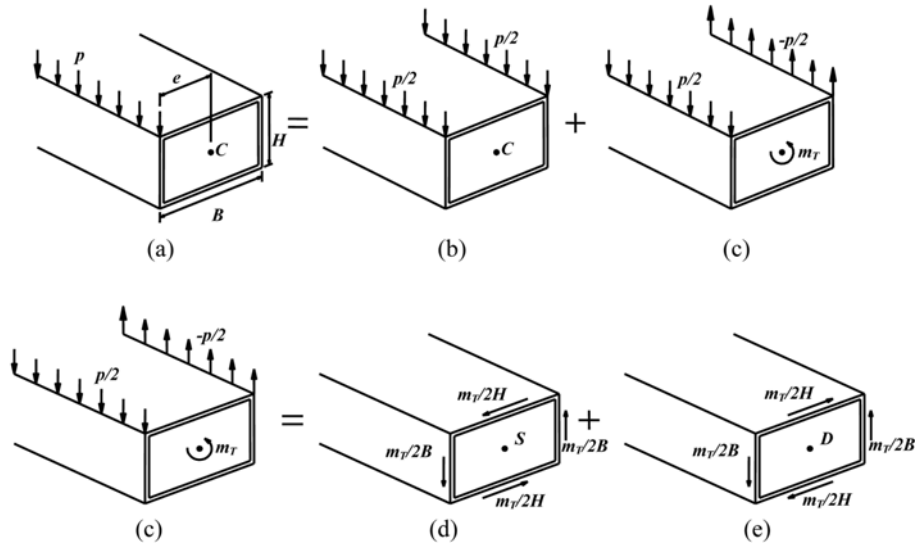


Fig. 1 Single-cell box girder subjected to an eccentric load (Nakai and Yoo 1988); (a) An eccentric load, (b) Flexure, (c) Torsion, (d) Pure torsion, (e) Distortional warping

causing flexure and torsion, respectively, and then the resolved torsional forces are again converted into pure torsional and distortional forces causing pure torsion and distortional warping, respectively (Nakai and Yoo 1988). The symbols B , H , e , C , S , D , and m_T denote the width and the height of each cell, the eccentricity from the centerline of the box section, the centroid, the shear center, the distortional center, and the torque or the torsional force, respectively. However, due to the basic assumption on distortion (Nakai and Yoo 1988) that the shear strain due to distortion γ is considered to be infinitesimal ($\gamma = 0$), the distortional forces in Fig. 1(e) is regarded as the forces not causing pure distortion but distortional warping. In other words, the distortional behavior due to the

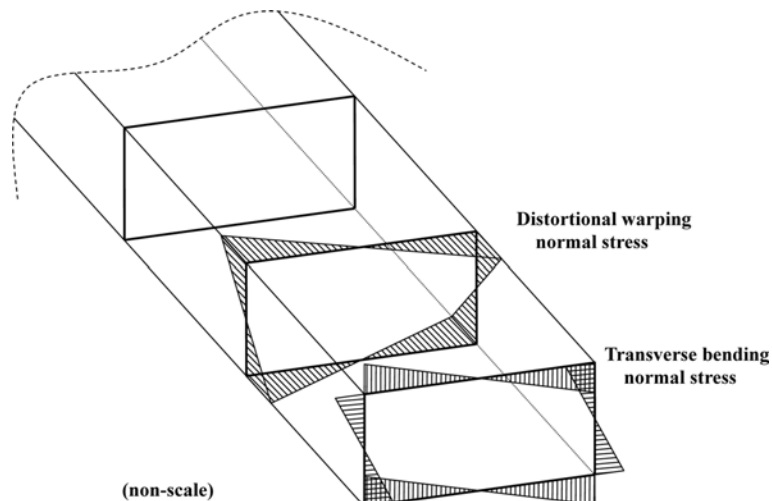


Fig. 2 Distributions of distortional warping normal and transverse bending normal stresses in a single-cell box girder

distortional forces can be divided into pure distortion and distortional warping, thus the zero shear strain assumption implies negligible pure distortional effect.

As a result, the distortional stress components occurring in single-cell box girders under an eccentric load are summarized as follows: the pure distortional shear stress, the distortional warping normal stress, the distortional warping shear stress, and the transverse bending normal stress. As aforementioned, the distortional warping normal stress and the transverse bending normal stress components in Fig. 2 are used among these four components when designing the intermediate diaphragm spacing of box girders.

3. Distortion of multicell box girders

An expanded method for independent analyses of multicell box girders using the shell elements is illustrated in this section in detail. This expanded method is defined as a force decomposition method of multicell box girders in this study, which is based on the methodology given by Nakai and Yoo (1988) in Sec. 2. In fact, in case of single-cell box girders, distortional forces inducing distortion are produced due to torsional forces only. However, in case of multicell box girders, the distortion inducing characteristics are somewhat different compared with those of single-cell box girders since forces inducing distortion of multicell box girders are caused by the flexural forces as well as the torsional forces. Distortional forces in multicell box girders are produced due to the following two reasons; one is to satisfy force equilibrium between the eccentric load and the flexural and torsional forces as shown in Figs. 3, 5 and 6 (designated here as “division process”), and the other is to satisfy force equilibrium between torsional forces as shown in Figs. 4 and 7 (designated here as “conversion process”).

Figs. 3 and 4 show graphically in detail the force decomposition processes (i.e., division and

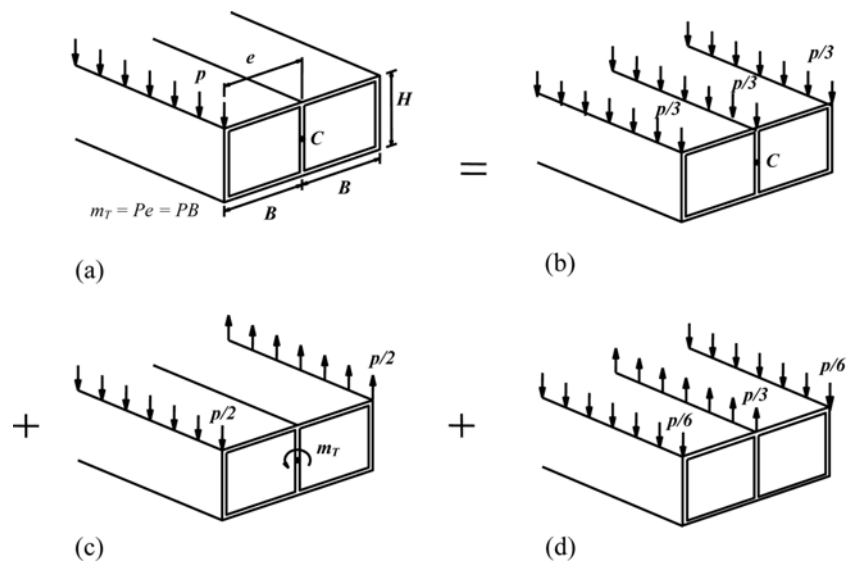


Fig. 3 Divided forces of an eccentric load (division process); (a) An eccentric load, (b) Flexural forces, (c) Torsional forces, (d) Distortional forces (2nd)

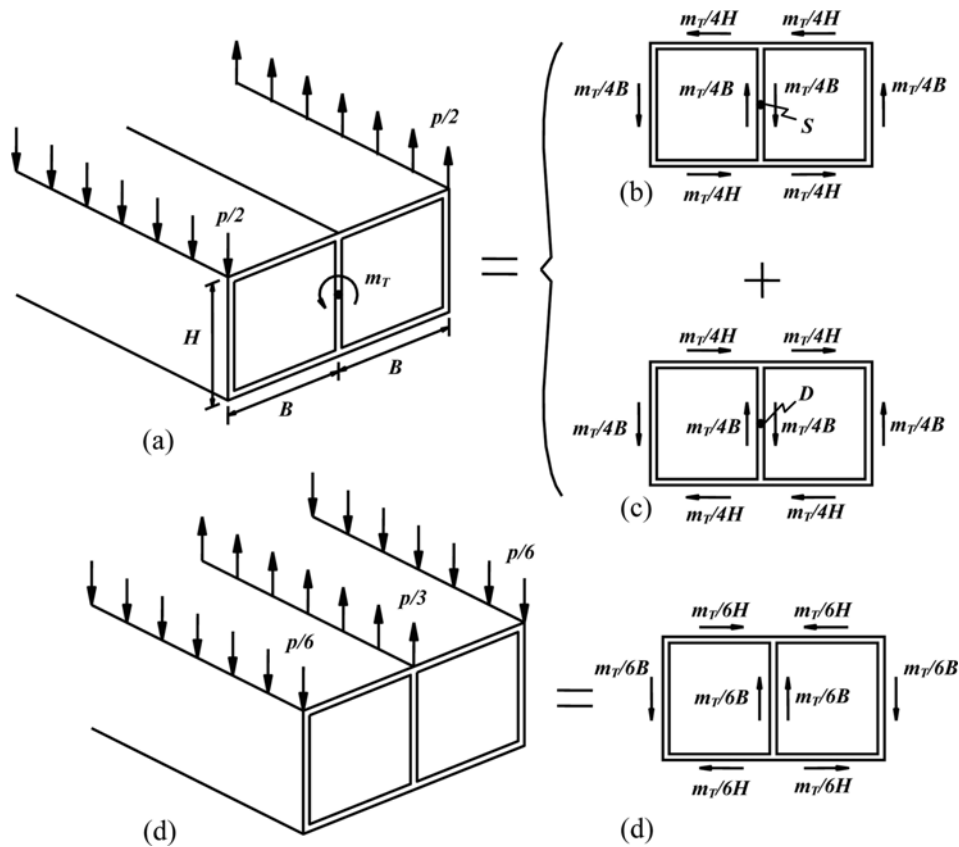


Fig. 4 Converted forces of torsional and distortional forces (conversion process); (a) Torsional forces, (b) Pure torsional forces, (c) Distortional forces (1st), (d) Distortional forces (2nd)

conversion processes) of a two-cell box girder subjected to an eccentric load. As shown in Fig. 3, the eccentric load p can be divided into the following three forces due to the division process: each flexural force of $p/3$ inducing flexure, each torsional force of $p/2$ inducing both pure torsion and the first mode distortion, and the second mode distortional forces of $p/6$ and $p/3$ inducing the second mode distortion. Subsequently, the divided forces, except the flexural forces, can be converted again into forces of $m_T/4B$, $m_T/4H$, $m_T/6B$, and $m_T/6H$ along the wall of the cross-section due to the conversion process, as shown in Fig. 4. Consequently, the four forces produce pure torsion and pure distortion of the two-cell box girder. Torsional warping and distortional warping can be produced in the two-cell box girder under the four forces if the box girder is restrained against warping at boundaries.

Meanwhile, when a three-cell box girder is subjected to an eccentric load on an outer web, divisions of the load can be considered as two cases depending on the location of applied torsional forces as shown in Figs. 5 and 6. In the first case where the torsional forces are applied to outer webs in Fig. 5(c), the flexural and the torsional forces are divided into $p/4$ for each web and $p/2$ for each outer web, respectively, and the second distortional forces are divided into $p/4$ for each web, as shown in Figs. 5(b) to 5(d). Also, similar to the two-cell box girders, the divided torsional forces can be converted into the pure torsional and the first mode distortional forces, as illustrated in

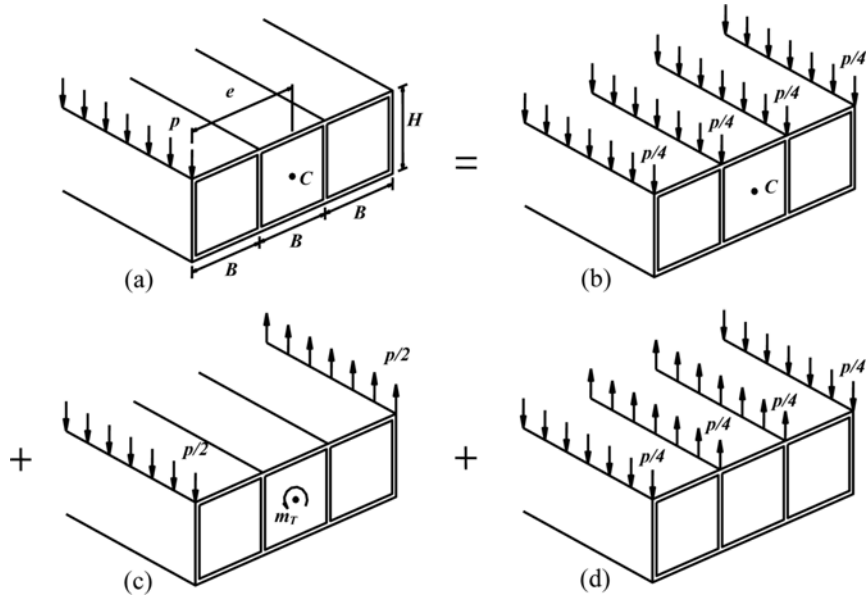


Fig. 5 Divided forces of an eccentric load (division process, first case); (a) An eccentric load, (b) Flexural forces, (c) Torsional forces, (d) Distortional forces (2nd)

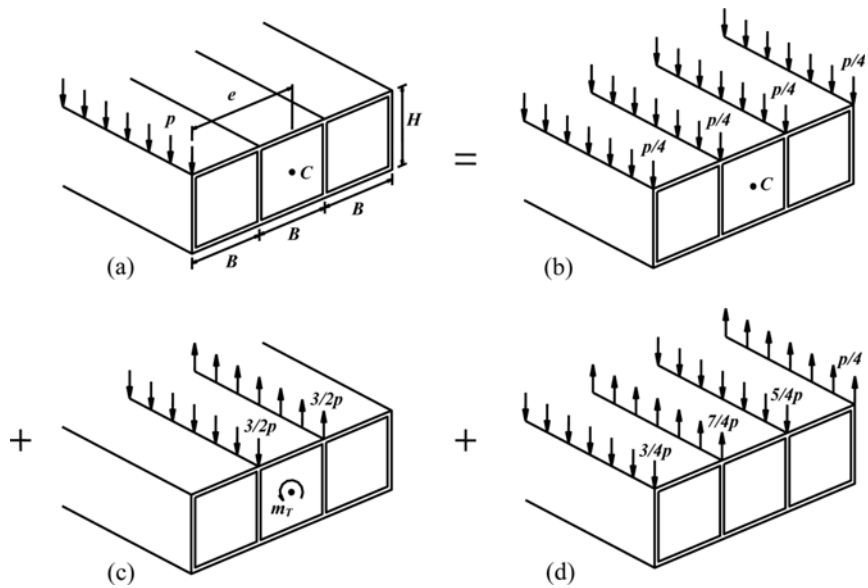


Fig. 6 Divided forces of an eccentric load (division process, second case); (a) An eccentric load, (b) Flexural forces, (c) Torsional forces, (d) Distortional forces (4th)

Figs. 7(a) to 7(c). As a result, the divided and the converted forces (i.e., the decomposed forces) produce the torsional and the distortional responses of the three-cell box girder.

Similar to the first case, in the second case where the torsional forces are applied to inner webs in Fig. 6(c), the flexural and the torsional forces are divided into $p/4$ for each web and $3p/2$ for each

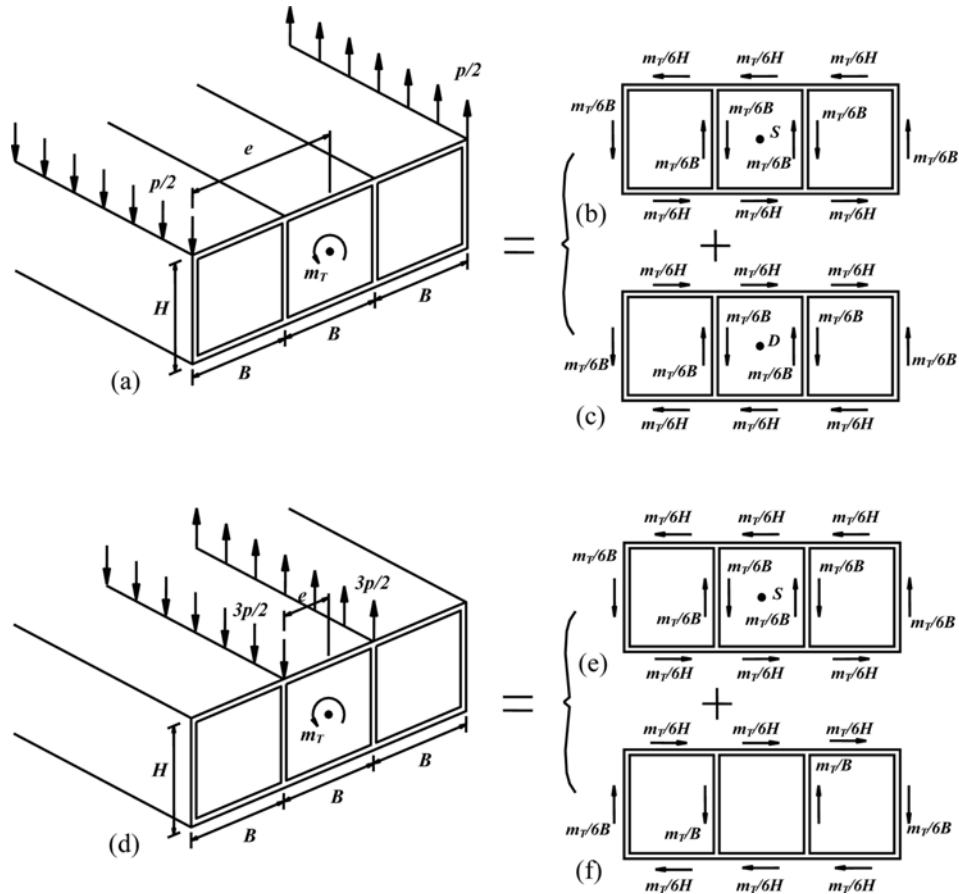


Fig. 7 Converted forces of torsional forces: First case; (a) Torsional forces, (b) Pure torsional forces, (c) Distortional forces (1st); Second case, (d) Torsional forces, (e) Pure torsional forces, (f) Distortional forces (3rd)

inner web, respectively, and the fourth mode distortional forces are divided into asymmetrically as shown in Figs. 6(b) to 6(d). The divided forces can be converted again into the pure torsional and the third mode distortional forces as shown in Figs. 7(d) to 7(f).

Meanwhile, when an additional eccentric load q is applied to an inner web of the three-cell box girder shown in Fig. 5, four additional decomposed distortional forces (designated here as “the 5th to the 8th forces”) are produced following the same processes (i.e., division and conversion processes).

In summary, it is evident from the expanded method that total numbers of the decomposed distortional forces of the two-cell box and the three-cell box girders are two forces (i.e., 1st, 2nd) and four forces (i.e., 1st, 2nd, 5th, 6th, or 1st, 2nd, 7th, 8th, or 3rd, 4th, 5th, 6th, or 3rd, 4th, 7th, 8th), respectively. Therefore, total distortional responses of the two-cell box girder, i.e., total distortional displacements and stresses, are simply obtained by superposition of separate distortional responses due to the 1st and the 2nd mode distortional forces in Figs. 4(c) and 4(d). Similarly, total distortional responses of the three-cell box girder are also obtained by superposition of separate distortional responses due to the four forces.

4. Superposition of independent distortional results

Total numbers of distortion of single-cell to five-cell box girders subjected to eccentric loads are expressed as the following equation by using the expanded method.

$$ND = \begin{cases} 2^{n-1} & (n = 1, 2, 3, 4) \\ 18 & (n = 5) \end{cases} \quad (1)$$

where the symbols ND and n denote the total numbers of distortional modes and the total cell numbers in box girders, respectively. For example, in case of the three-cell box girder, the total numbers of distortional modes are easily calculated as $2^{3-1} = 4$. The four distortional modes are produced due to four distortional forces decomposed from eccentric loads p and q , as mentioned in Sec. 3. In this study, the number of cell is limited to five since the six or more cells are not practical in most box girder bridges. However, the ND can be enlarged into the more multicell box girders by using the expanded method.

Based on the expanded method, total distortional responses of multicell box girders are readily obtained by superposing independent distortional responses. For example, when an eccentric load of 100 kN/m (i.e., $p = 100$ kN/m) is applied to a two-cell box girder as shown in Fig. 8(a), the load decomposes into the 1st and the 2nd mode distortional forces in Figs. 8(b) and 8(c), thus the total distortional results are obtained by superposition of independent distortional responses under the 1st and the 2nd mode distortional forces. Similarly, when an eccentric load of 200 kN/m (i.e., $p = 200$ kN/m and $q = 0$ kN/m) is applied to a three-cell box girder as shown in Fig. 9(a), total distortional results are obtained by superposition of independent distortional responses under the 1st and the 2nd mode distortional forces in Figs. 9(b) and 9(c), or under the 3rd and the 4th mode distortional forces in Figs. 9(d) and 9(e).

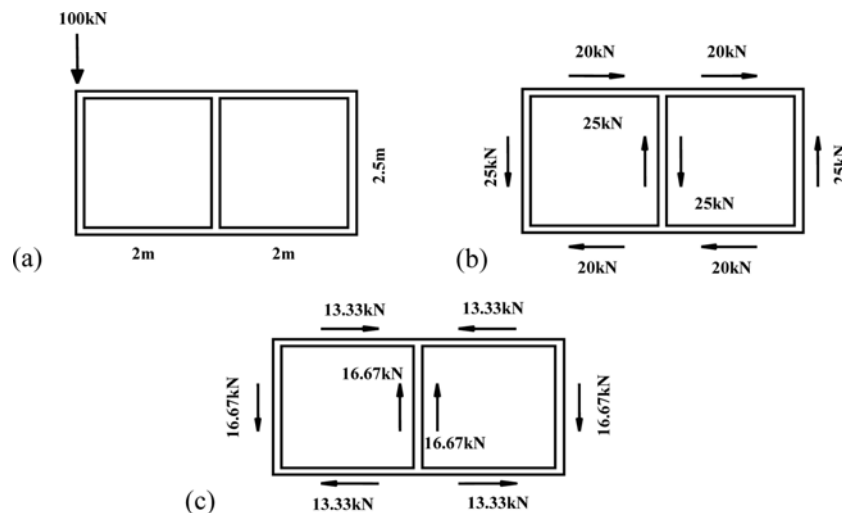


Fig. 8 Decomposed distortional forces of a two-cell box girder; (a) An eccentric load (center-to-center distances), (b) Distortional forces (1st), (c) Distortional forces (2nd)

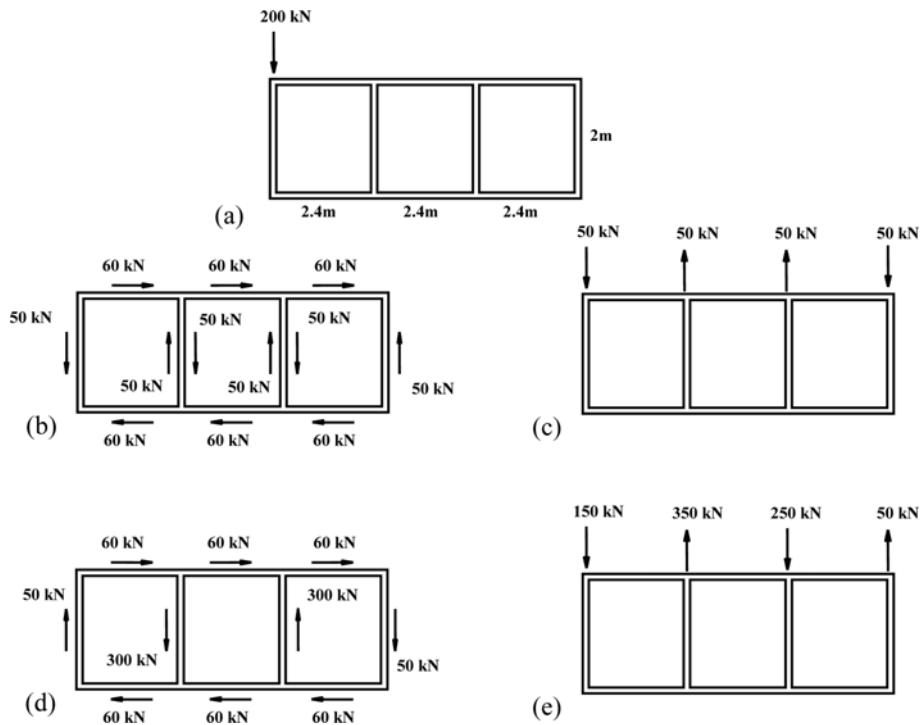


Fig. 9 Decomposed distortional forces of a three-cell box girder; (a) An eccentric load (center-to-center distances), (b) Distortional forces (1st), (c) Distortional forces (2nd), (d) Distortional forces (3rd), (e) Distortional forces (4th)

5. Numerical examples for independent analysis methods

Three box girder bridge models were selected to validate the proposed expanded method. The finite element program used for analyses of the three models is LUSAS (1999) that is one of the conventional finite element programs. The selection of models used for comparative studies is extremely difficult since most of the models of box girders used in the other previous studies reported up to date were limited to the straight/curved/skewed box girders with a trapezoidal cross-section except two straight two-cell box girder bridge models with a rectangular cross-section given by Zhang and Lyons (1984) and Willam and Scordelis (1972). Therefore, the straight two-cell box girder model given by Zhang and Lyons (1984) was selected herein in addition to two other hypothetical models of single-cell and three-cell box girder bridges.

The proposed expanded method is carried out in the following order; first, an eccentric load is decomposed into flexural, torsional and distortional forces; secondly, based on each force decomposition, each analysis using the shell elements is carried out; finally, the total distortional responses are obtained by superposition of independent distortional responses, whereas the total flexural and total torsional results are directly obtained by independent flexural and independent torsional analyses, respectively.

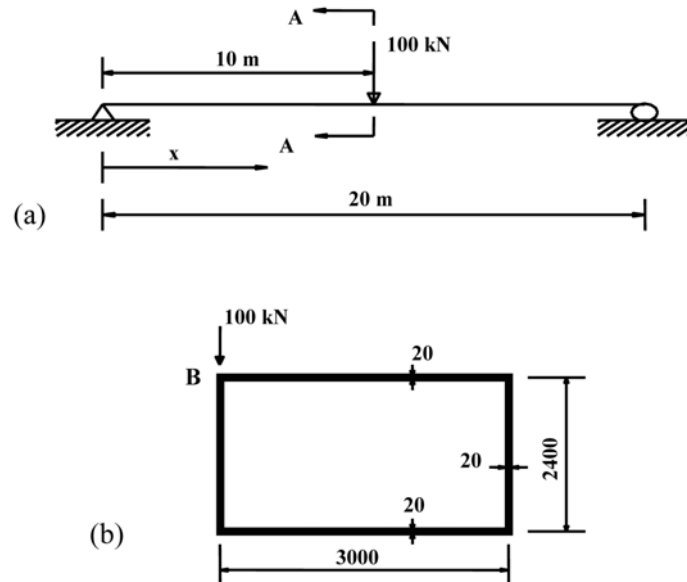


Fig. 10 Geometric and load descriptions of the first model; (a) Elevation, (b) Cross-section A-A (unit: mm)

5.1 A single-cell box girder bridge model

A single-span steel-box girder bridge model with a single-cell cross-section in Fig. 10 was selected to validate the proposed expanded method. This model is subjected to a concentrated load of 100 kN at point B of the mid-span as shown in Fig. 10. Therefore, the torsional force or the torque is calculated as $150 \text{ kN} \cdot \text{m}$. A bearing diaphragm having thickness of 20 mm is installed at both supports of this model. The modulus of elasticity and the Poisson's ratio are 210000 MPa and 0.3, respectively. The total number of shell elements used for each independent analysis is 7200. The shell elements of the LUSAS (1999) have six degrees of freedom per node and have four nodes per element.

The proposed method begins with the decomposition of the eccentric load of 100 kN, as shown in Fig. 11. Subsequently, based on each decomposition as shown in Figs. 11(b) to 11(d), each separate analysis using the shell element is performed.

In order to verify the proposed method, seven analyses are carried out for the model herein: the first is the independent flexural analysis under the decomposed flexural forces in Fig. 11(b), the second the independent torsional analysis under the decomposed pure torsional forces in Fig. 11(c), the third the independent distortional analysis under the decomposed pure distortional forces in Fig. 11(d), the fourth the combined analysis under the concentrated eccentric load in Fig. 11(a), the fifth the combined analysis under the distributed eccentric load, the sixth the combined analysis using a single-cell box beam element developed by Park *et al.* (2003) under the eccentric load, and the last the distortional analysis using the box element developed by Park *et al.* (2003) under the pure distortional forces in Fig. 11(d). When performing four analyses except the fourth, the sixth, and the last, the decomposed concentrated forces and the concentrated eccentric load are changed into distributed forces per unit web-length for the sake of preventing any possible local behavior. For example, in case of the fifth analysis, the concentrated eccentric load of 100 kN is changed into

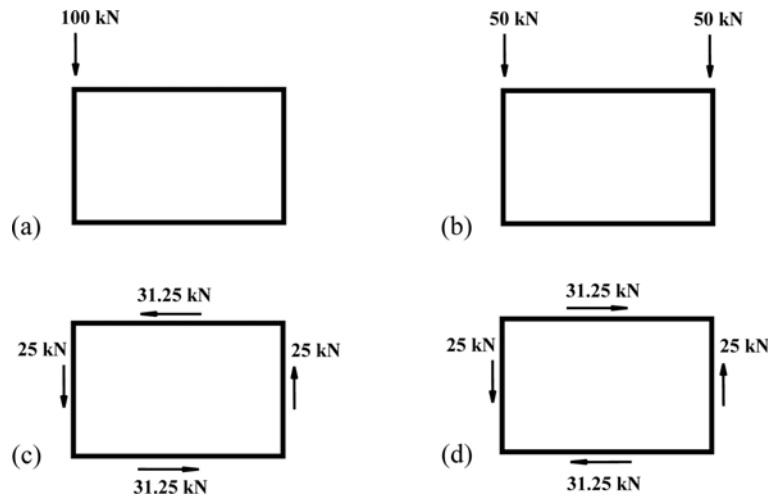


Fig. 11 Decomposed forces of the first model; (a) An eccentric load, (b) Flexural forces, (c) Pure torsional forces, (d) Distortional forces (1st)

the distributed eccentric load of $100 \text{ kN}/2.4 \text{ m} = 41.667 \text{ kN/m}$ and then is applied to an outer web.

Separate analysis results corresponding to types of applied forces are shown in Figs. 12 to 14. Indexes in parenthesis in Figs. 12 to 14, i.e., F, Pt, Pd, EL, EL(D), and F + Pt + Pd denote the decomposed flexural forces, the decomposed pure torsional forces, the decomposed pure distortional forces, the concentrated eccentric load, the distributed concentrated load, and the sum of the forces related to the decomposed flexural, the decomposed pure torsional, and the decomposed pure distortional forces, respectively. Figs. 12 and 13 show the maximum vertical displacements and the maximum normal stresses at B along the span length. It is evident from Figs. 12 and 13 that the

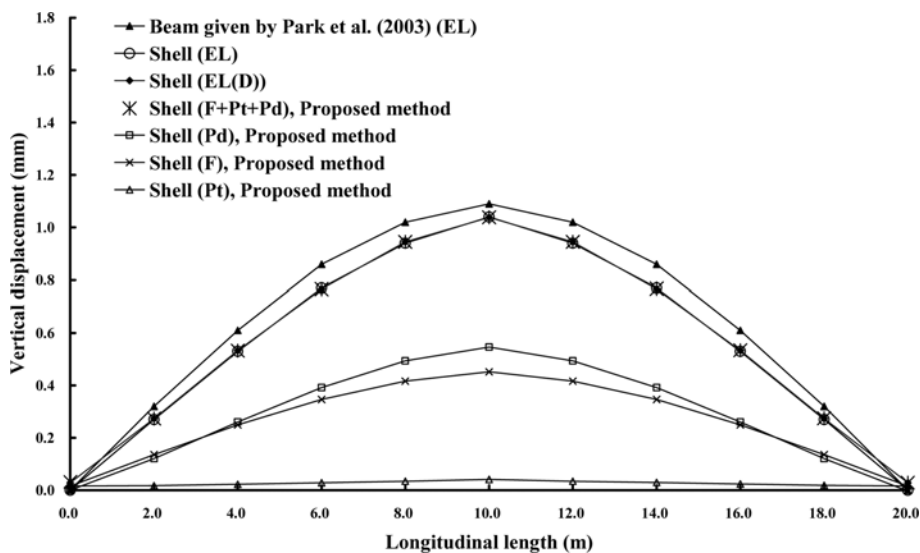


Fig. 12 Vertical displacements of the first model at B along the span length (unit: mm)

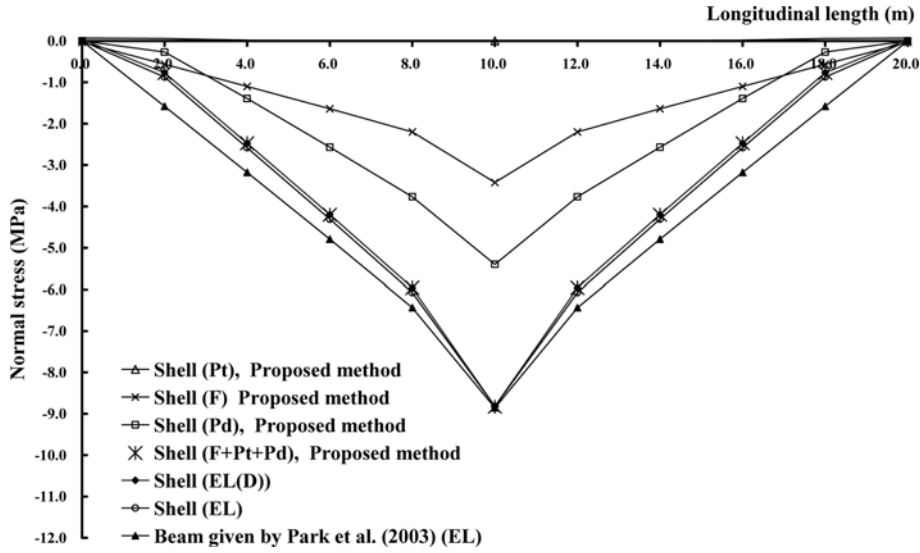


Fig. 13 Normal stresses of the first model at B along the span length (unit: MPa)

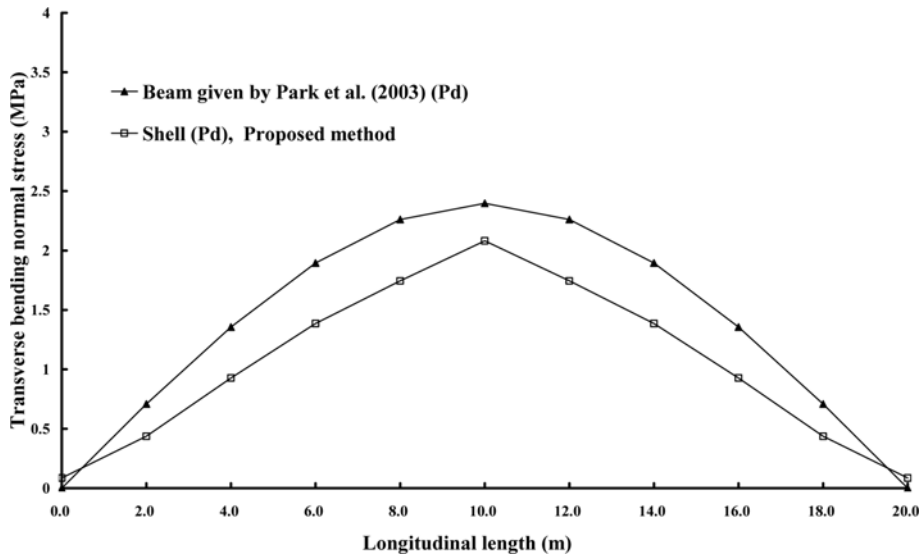


Fig. 14 Transverse bending normal stresses of the first model at B along the span length (unit: MPa)

displacements and stresses due to F + Pt + Pd are practically equal to those due to EL(D) and EL. This strongly supports the validity of the proposed method.

5.2 A two-cell box girder bridge model

The second model selected for validity of the proposed expanded method was a two-span concrete-box girder bridge model with a two-cell rectangular cross-section given by Zhang and Lyons (1984) in Fig. 15. This model is subjected to two concentrated loads of 10 kN acting on the

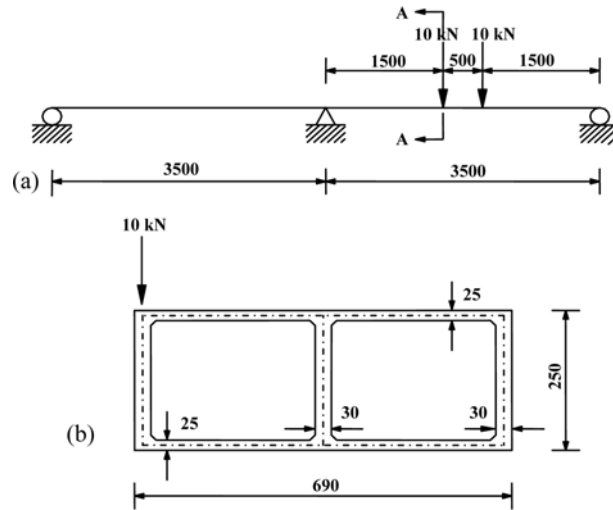


Fig. 15 Geometric and load descriptions of the second model (Zhang and Lyons 1984); (a) Elevation (unit: mm), (b) Cross-section A-A (unit: mm)

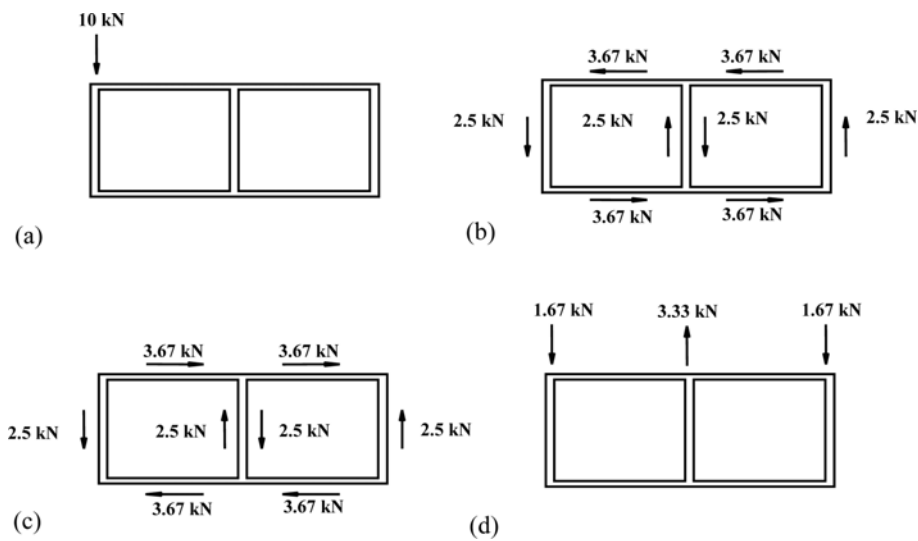


Fig. 16 Decomposed forces of the second model; (a) An eccentric load, (b) Pure torsional forces, (c) Distortional forces (1st), (d) Distortional forces (2nd)

second span, thus the torque is calculated as 3.3 kN · m. This model is assumed to have no bearing and intermediate diaphragms. The modulus of elasticity and the Poisson's ratio of this model are assumed as 29000 MPa and 0.18, respectively. They used 188 shell elements for the general shell analysis whereas 3920 shell elements for the independent analyses were employed herein for accuracy.

In order to obtain separate analysis results of this model, the eccentric load is decomposed into flexural, torsional and distortional forces based on the expanded method, as shown in Fig. 16. The decomposed flexural forces are omitted from Fig. 16 since the forces are similar to those of the single-cell box girder. Subsequently, the individual separate analyses based on the decomposed

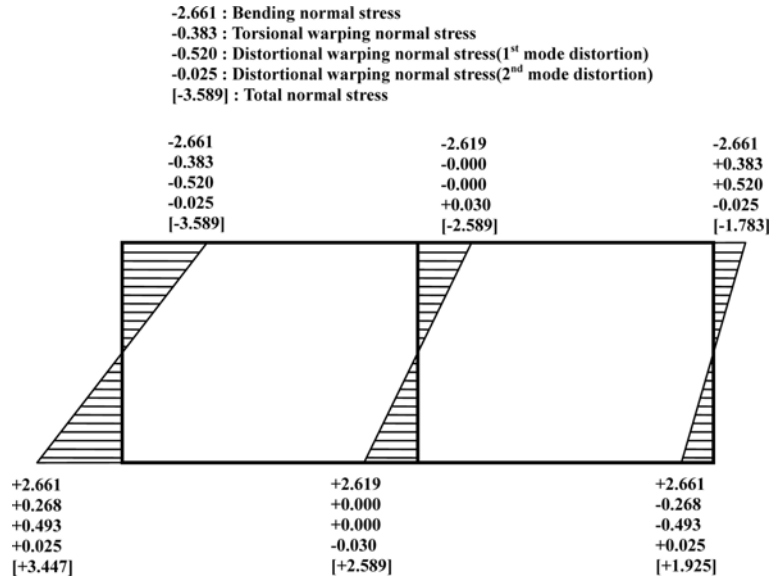


Fig. 17 Normal stress distributions of the second model due to the proposed method at the mid-span section of the second span (unit: MPa)

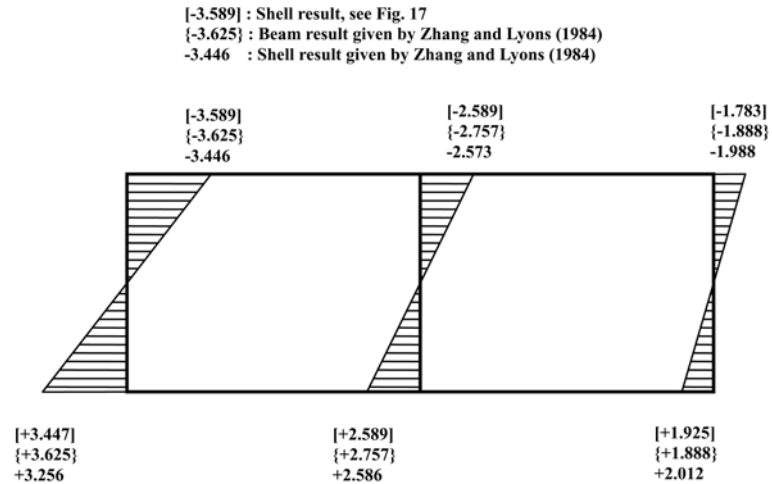


Fig. 18 Normal stress distributions of the second model according to each analysis method at the mid-span section of the second span (unit: MPa)

forces are performed herein (see Fig. 17). Unfortunately, stress outputs given by Zhang and Lyons (1984) regarding this model were the normal stresses only at the mid-span section of the second span. Therefore, the normal stresses are compared with each other in this study as shown in Fig. 18. Plus and minus signs in Figs. 17 and 18 denote tensile and compressive stresses, respectively. It is evident from Figs. 17 and 18 that total normal stresses due to the proposed method, i.e., the sum of each normal stress shows a good correlation with the normal stresses given by Zhang and Lyons (1984). This also strongly supports the validity of the proposed expanded method.

5.3 A three-cell box girder bridge model with intermediate diaphragms

The third model is a single-span three-cell steel-box girder bridge model with two intermediate diaphragms shown in Fig. 19. Since analytical and experimental results of box girder models with a three-cell rectangular section are not currently available, any comparison with other study is not possible either. This model is subjected to an eccentric load of 200 kN (i.e., $p = 200$ kN and $q = 0$) at B of the mid-span section thus the torque is calculated as 720 kN · m. This model has two

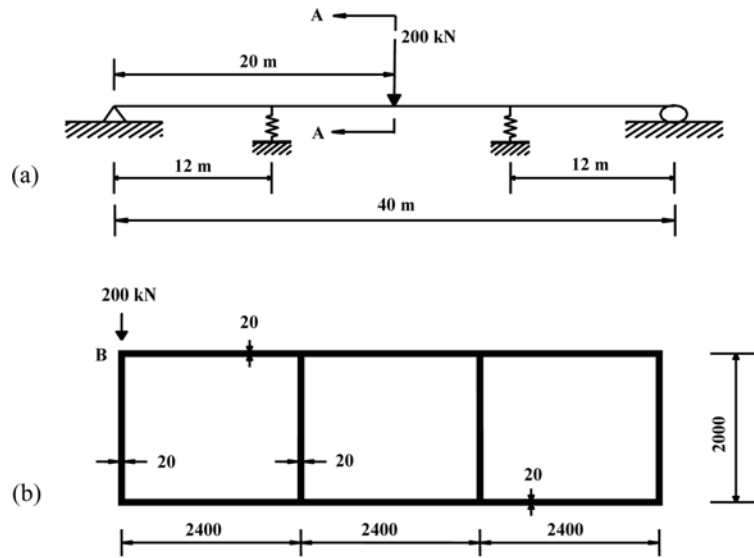


Fig. 19 Geometric and load descriptions of the third model; (a) Elevation, (b) Cross-section A-A (unit: mm)

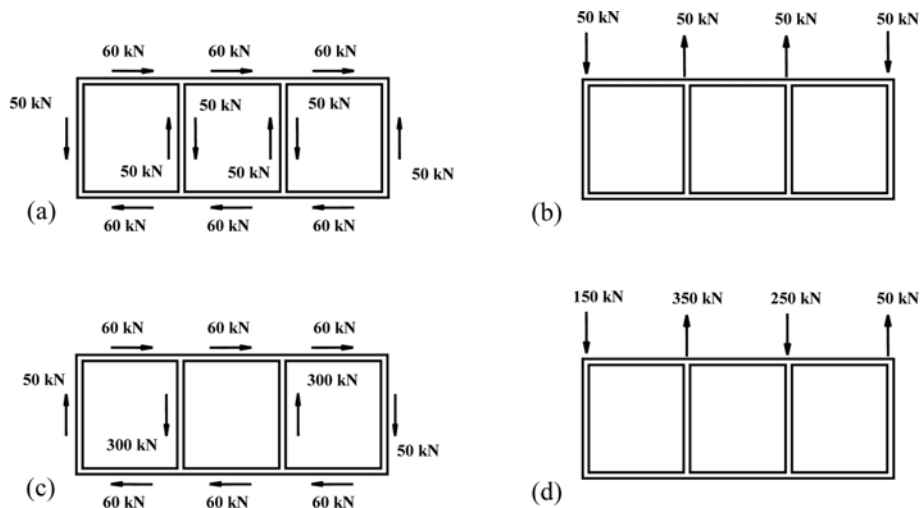


Fig. 20 Decomposed distortional forces of the third model; (a) Distortional forces (1st), (b) Distortional forces (2nd), (c) Distortional forces (3rd), (d) Distortional forces (4th)

bearing and two intermediate diaphragms of 30 mm thickness. The modulus of elasticity and the Poisson's ratio are assumed as 210000 MPa and 0.3, respectively. The total number of shell elements used for each independent distortional analysis is 12000. The elements have four nodes per element and six degrees of freedom per node.

Figs. 21 to 23 show vertical displacements, distortional warping normal stresses, and transverse bending normal stresses of this model at B along the span length, respectively. The results are due to four independent distortional analyses corresponding to the decomposed distortional forces in Fig. 20. Among the indexes in Figs. 21 to 23, total distortion (1st + 2nd) and total distortion (3rd + 4th) denote the sum (or superposition) of results due to the 1st and the 2nd mode distortional analyses,

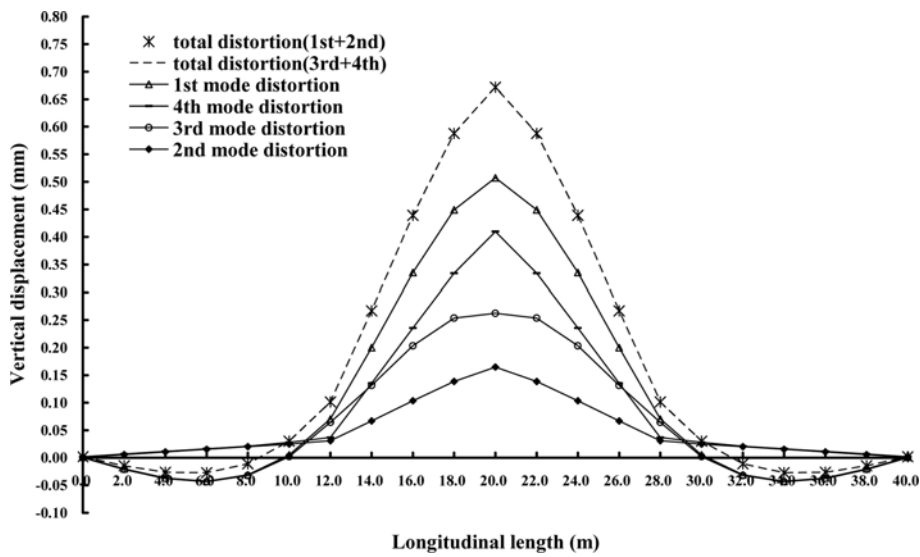


Fig. 21 Vertical displacements of the third model at B along the span length (unit: mm)

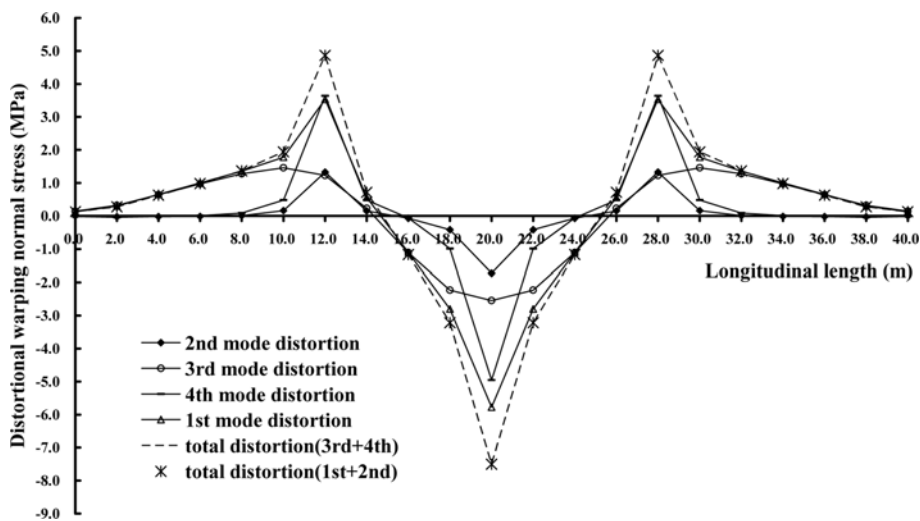


Fig. 22 Distortional warping normal stresses of the third model at B along the span length (unit: MPa)

and the sum of results due to the 3rd and the 4th mode distortional analyses, respectively. It is evident from Figs. 21 to 23 that total distortional results due to the 1st and the 2nd mode distortion show an excellent correlation with those due to the 3rd and the 4th mode distortion.

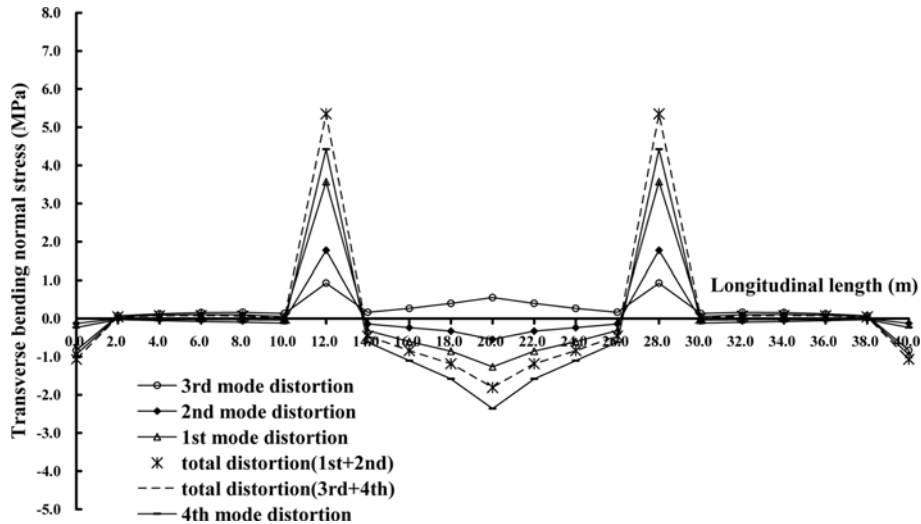


Fig. 23 Transverse bending normal stresses of the third model at B along the span length (unit: MPa)

Table 1 Values of normal stresses due to both the proposed method and the general shell analysis method

Type of methods	Type of forces	Normal stresses (MPa)		Figures (forces)	
		1 st case in Fig. 5	2 nd case in Fig. 6		
Proposed method	Flexural forces	-6.673	-6.673	Fig. 5(b)	
	Pure torsional forces	-0.312	-0.312	Fig. 7(b) or 7(e)	
	Pure distortional forces	1 st	-5.766	-	Fig. 20(a)
		2 nd	-1.724	-	Fig. 20(b)
		1 st + 2 nd	-7.490	-	-
		3 rd	-	-2.549	Fig. 20(c)
		4 th	-	-4.941	Fig. 20(d)
	3 rd + 4 th	-	-7.490	-	
	Sum of each forces		-6.673	-6.673	
			-0.312	-0.312	
		-7.490	-7.490	-	
		= -14.475	= -14.475		
General shell analysis method	An eccentric load	-14.475		Fig. 19(b)	

Note: (+) tensile stress, (-) compressive stress

Table 1 shows values of normal stresses due to both the proposed method under the decomposed forces and the general shell analysis method under an eccentric load at B of the mid-span section. As shown in Table 1, value of total normal stress due to the first case in Figs. 5(b), 7(b), 20(a), and 20(b), -14.475 MPa, is exactly the same as that due to the second case shown in Figs. 5(b), 7(b), 20(c), and 20(d). Also, value of normal stress due to the general shell analysis method, -14.475 MPa, is also exactly equal to that due to the proposed method. This shows also the validity of the proposed method.

Among the stress components due to the proposed method, the shear stresses are not discussed in Sec. 5 since the major stress components in box girder bridges with a closed cross-section are the normal stresses such as bending and warping normal stresses. It should be noted that the shear stresses can also be easily obtained, if necessary, based on the proposed method.

6. Conclusions

An expanded method in which individual responses of flexure, torsion, and distortion of multicell box girders subjected to an eccentric load could be taken into account was proposed in this study. Based on the proposed expanded method, independent analysis methods of multicell box girders are systematically proposed as follows: first, using the expanded method, an eccentric load is decomposed into flexural, torsional and multimode distortional forces before performing each analysis; secondly, based on the decomposed forces, each independent analysis using the existing shell elements is carried out; finally, total distortional results are obtained by superposition of independent distortional analysis results, whereas total flexural and total torsional results are directly obtained by independent flexural and independent torsional analyses, respectively. In addition, total numbers of distortion of multicell box girders were evaluated in Eq. (1) using the expanded method, which gives significant information for better physical understanding of distortional phenomenon of multicell box girders.

Three box girder bridge models were selected to verify the validity of the expanded method. It is evident from comparative studies that displacements and stresses due to both the general shell analysis method and the proposed expanded method show an excellent correlation with each other, which strongly supports the validity of the proposed expanded method.

Since no preliminary estimation of section-properties such as the distortional center, the distortional warping function, the distortional stiffness, and so on, is necessary, the proposed expanded method is evidently a very useful and convenient resort for practicing engineers. In addition, noting that the spacing requirement of intermediate diaphragms is based on the limiting ratio of the distortional warping normal stress to the bending normal stress and the limiting value of the transverse bending normal stress, accurate and convenient analysis method in which the distortion related responses can be separately obtained from other responses such as bending and torsion is of paramount importance for practicing engineers.

Acknowledgements

This work was one of researches for the NRL-Establishment of Structural Technology for Future Railway system, which was supported by the Korea Science and Engineering Foundation Grant funded by the Korean Government (MOST).

References

- Dabrowski, R. (1968), *Curved Thin-Walled Girders Theory and Analysis*, Cement and Concrete Association.
- Guide Specifications for Horizontally Curved Highway Bridges (1993), American Association of State Highway and Transportation Officials (AASHTO), Washington D.C.
- Guidelines for the Design of Horizontally Curved Girder Bridges (1988), Hanshin Expressway Public Corporation, Japan.
- Jonsson, J. (1999), "Distortional theory of thin-walled beams", *Thin-Walled Structures*, **33**, 269-303.
- LUSAS Finite Element Analysis System, User's Manual (1999), Finite Element Analysis Ltd., London, UK.
- Maisel, B.I. (1970), *Review of Literature Related to the Analysis and Design of Thin-Walled Beams*, Cement and Concrete Association, Technical Report 440, London, UK.
- Maisel, B.I. (1985), "Analysis of concrete box beams using small computer capacity", *Canadian J. of Civil Engineering*, **12**, 265-278.
- Nakai, H. and Yoo, C.H. (1988), *Analysis and Design of Curved Steel Bridges*. McGraw-Hill, New York, 111-117.
- Park, N.H., Lim, N.H. and Kang, Y.J. (2003), "A consideration on intermediate diaphragm spacing in steel box girder bridges with a doubly symmetric section", *Eng. Struct.*, **25**(13), 1665-1674.
- Razaqpur, A.G. and Li, H.G. (1991), "Thin-walled multicell box-girder finite element", *J. Struct. Eng.*, ASCE, **117**(10), 2953-2971.
- Razaqpur, A.G. and Li, H.G. (1994), "Refined analysis of curved thin-walled multicell box girders", *Comput. Struct.*, **53**(1), 131-142.
- Sedlacek, G. (1968), *Systematic Description of the Process of Bending and Torsion for Prismatic Beams of Thin-Walled Cross-Section Considering Distortion of Cross-Section*. Fortschritt-Berichte VDI-Zeitschrift, Reihe 4, Nr. 8, Sept., (In Germany).
- Willam, K.J. and Scordelis, A.C. (1972), "Cellular structures of arbitrary plan geometry", *J. Struct. Div.*, ASCE, **98**(7), 1377-1394.
- Zhang, S.H. and Lyons, L.P.R. (1984), "A thin-walled box beam finite element for curved bridge analysis", *Comput. Struct.*, **18**(6), 1035-1046.